Refined 1.8 Å structure of human aldose reductase complexed with the potent inhibitor zopolrestat

(active site/diabetic complications/drug design)

DAVID K. WILSON*, IVAN TARLE†, J. MARK PETRASH†, AND FLORANTE A. QUIOCHO*‡

*Howard Hughes Medical Institute and Departments of Biochemistry and Molecular Physiology and Biophysics, Baylor College of Medicine, Houston, TX 77030; and †Departments of Ophthalmology and Visual Sciences and Genetics, Washington University School of Medicine, St. Louis, MO 63110

ABSTRACT As the action of aldose reductase (EC 1.1.1.21) is believed to be linked to the pathogenesis of diabetic complications affecting the nervous, renal, and visual systems, the development of therapeutic agents has attracted intense effort. We report the refined 1.8 Å x-ray structure of the human holoenzyme complexed with zopolrestat, one of the most potent noncompetitive inhibitors. The zopolrestat fits snugly in the hydrophobic active site pocket and induces a hinge-flap motion of two peptide segments that closes the pocket. Excellent complementarity and affinity are achieved on inhibitor binding by the formation of 110 contacts ($\leq$4 Å) with 15 residues (10 hydrophobic), 13 with the NADPH coenzyme and 9 with four water molecules. The structure is key to understanding the mode of action of this class of inhibitors and for rational design of better therapeutics.

Aldose reductase (ALR2; EC 1.1.1.21) is an NADPH-dependent enzyme that catalyzes the reduction of a wide variety of carbonyl-containing compounds to their corresponding alcohols. Although its cellular role is not established, it catalyzes the first and rate-limiting step of the polyol pathway of glucose metabolism. The catalytic efficiency of ALR2 varies widely for different substrates, but it shows a marked preference for hydrophobic compounds (1) consistent with the discovery of a highly hydrophobic active site pocket (2) and evidence that aldose reductase and steroid dehydrogenase activities are manifested by the same gene product (3).

Clinical interest in ALR2 has been raised by its ability to reduce glucose to sorbitol. Enhanced flux of glucose through the polyol pathway is believed to be linked to a number of diabetic complications, including neuropathy, nephropathy, and retinopathy (4–6). Since glucose is an extremely poor substrate, this accumulation is not usually significant except in patients with diabetes mellitus and chronic hyperglycemia. A very large number of heterocyclic inhibitors of ALR2 have been and continue to be developed and some have shown promise in the treatment of diabetic complications (7).

There are two major classes of these inhibitors characterized by a structural or functional group present—spirohydantoins and carboxylic acids (5–7). Inhibition and competition studies suggest that these compounds bind at a site independent of the substrate and coenzyme (5, 6). One recent and promising (in vitro and in vivo) carboxylic acid inhibitor is zopolrestat (3,4-dihydro-4-oxo-3-{[5-(trifluoromethyl)-2-benzothiazolyl]methyl}-1-phthalazineacetic acid, compound 1 with atom numbers based on its crystal structure) (8). Besides displaying an IC50 of 3 nM (8), zopolrestat exhibits excellent pharmacokinetic properties in humans and is currently in Phase II clinical studies (7). Kinetic studies of zopolrestat, using a purified recombinant human ALR2 (9),

1
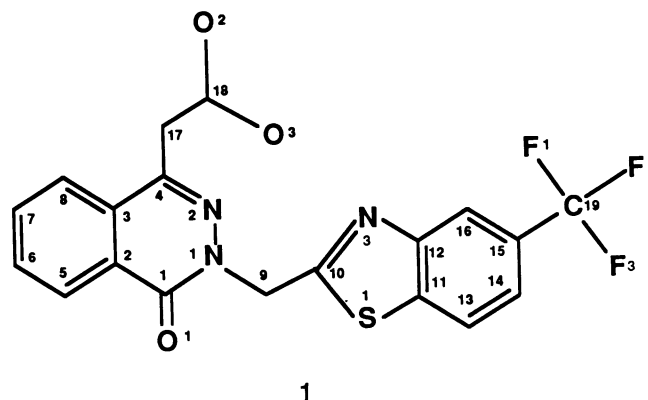
showed mixed-type noncompetitive inhibition with values of 5.5 nM and 8.4 nM for the uncompetitive and noncompetitive inhibition constants, respectively (J.M.P. and T. H. Harter, unpublished data).

Here we describe the crystal structure of the ternary complex of human ALR2 with coenzyme and zopolrestat refined at 1.8 Å resolution and compare it with the binary (enzyme–coenzyme) or holoenzyme structure, which we have recently determined to 1.4 Å resolution (D.K.W., J.M.P., and F.A.Q., unpublished data).§ Structures have also been previously determined for the porcine form (10) as well as a Cys-298 to Ser mutant of the human holoenzyme (11). The overall topology is preserved among all of these structures. The ALR2 structure belongs to the $(\beta/\alpha)_8$-barrel class of enzymes (the most prevalent motif for enzymes) and, to our knowledge, is the first of this class that binds an NAD(P). The coenzyme molecule is bound to the C-terminal end of the β barrel. In the holoenzyme structures, the nicotinamide moiety forms the base of a large active site pocket that is heavily lined by hydrophobic residues.

Materials and Methods

Human ALR2, encoded by a cDNA clone, was obtained by overexpression in *Escherichia coli* and purification as published (9). The purified enzyme was used to obtain crystals of the holoenzyme that was solved to 1.4 Å resolution (D.K.W., J.M.P., F.A.Q., unpublished data). Crystals of the holoenzyme–zopolrestat complex were grown using the hanging drop method. Drops containing 7 mg of ALR2 per ml, ≈200 μM zopolrestat, 3.5 mM 2-mercaptoethanol, and 25 mM citrate (pH 5.0) were suspended over wells of 17% polyeth-

Abbreviation: ALR2, aldose reductase.
‡To whom reprint requests should be addressed.
§The atomic coordinates have been deposited in the Protein Data Bank, Chemistry Department, Brookhaven National Laboratory, Upton, NY 11973 (reference 1MAR). This information is embargoed for 1 year (coordinates) from the date of publication.
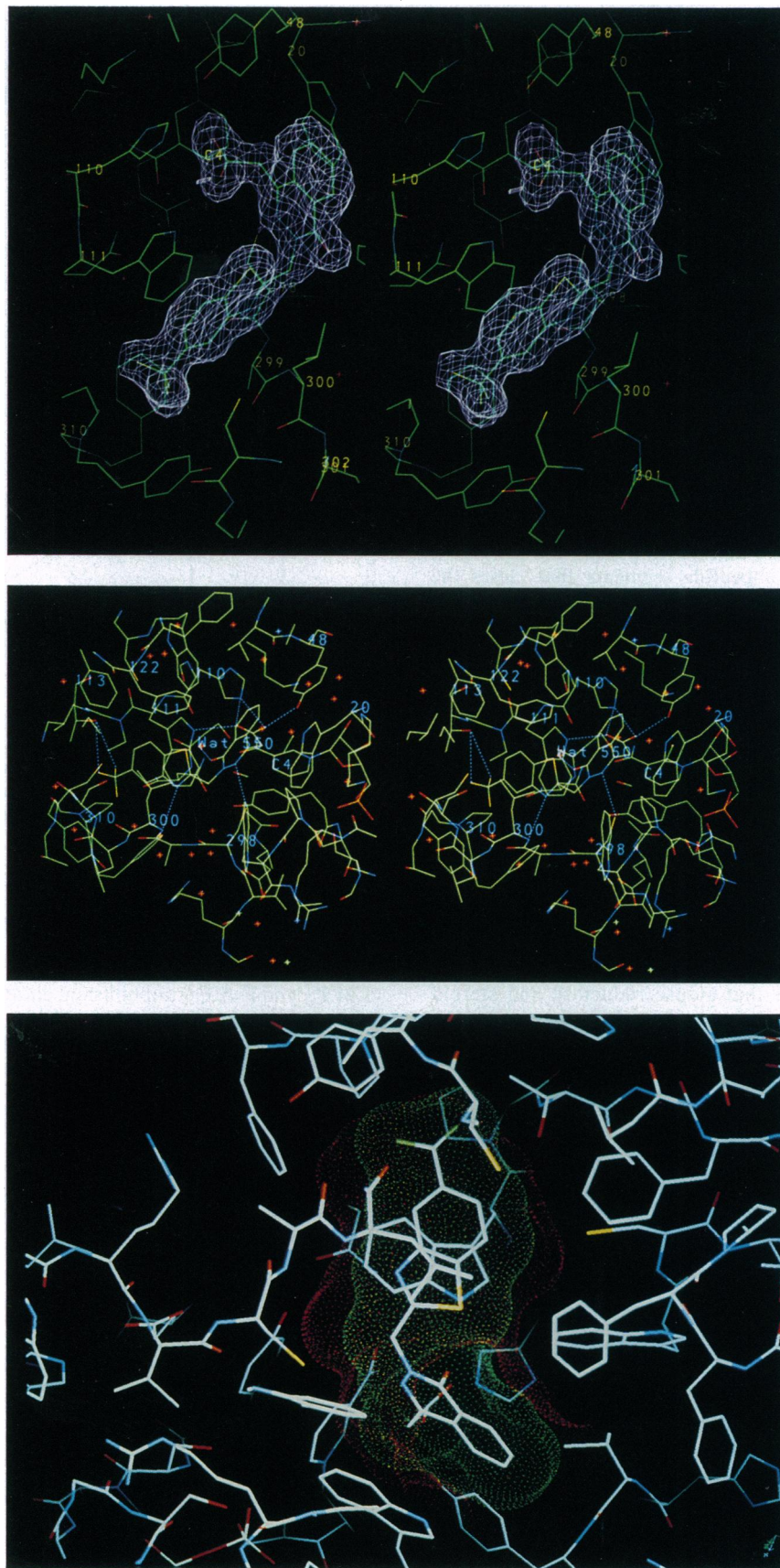
FIG. 1. Zopolrestat bound to ALR2. (*Top*) Difference electron density (magenta) of the zopolrestat and superimposed refined structure (atoms color coded). The density (contoured at 3σ) was calculated with coefficients ($|F_o| - |F_c|$) and α_c phases from the refined 1.8 Å structure with the inhibitor atoms omitted. The C4 atom of the nicotinamide ring of NADPH is identified as well as some residues involved in inhibitor binding and possibly in catalysis (Tyr-48 and His-110). (*Middle*) Hydrogen bonds (dashed lines) between the zopolrestat and enzyme.

Biochemistry: Wilson *et al.*

Proc. Natl. Acad. Sci. USA 90 (1993) 9849

ylene glycol 6000, 7 mM 2-mercaptoethanol, and 50 mM citrate (pH 5.0). A different crystal morphology than those of the holoenzyme crystals indicated a possible new crystal form. The diffraction data set from 20 Å to 1.8 Å resolution was collected on a Rigaku R-Axis area detector mounted on a rotating anode generator equipped with a graphite mono-chromator and operated at 50 kV and 90 mA. The indexing of this data set indicated a space group of $P1$ and a unit cell with dimensions of $a = 47.64$ Å, $b = 48.04$ Å, $c = 40.48$ Å, $\alpha = 67.47°$, $\beta = 76.77°$, and $\gamma = 76.07°$ and a content of one enzyme molecule. Merging of 53,037 measured reflections resulted in an R-merge of 0.034 (based on intensity) and 26,145 unique reflections (90.4% complete). In the structure determination we used 25,891 reflections with $F \geq 1\sigma(F)$ between 12 Å and 1.8 Å resolutions.

The structure of the ternary complex was determined by molecular replacement (12) using the refined 1.4 Å holoenzyme structure (solvent molecules omitted) as a search model. Rotation function and structure refinement were carried out using the X-PLOR suite of programs (13). The angles defining the highest rotation peak ($\theta_1 = 48°$, $\theta_2 = 84°$, and $\theta_3 = 90°$) in the rotation search using amplitudes between 20 Å and 6 Å were applied directly to the model without any Patterson-correlation refinement. After several cycles of rigid body refinement, using reflections between 12 Å and 4 Å, the crystallographic R-factor [$= (\Sigma||F_o| - |F_c||/\Sigma|F_o|)$] decreased from an initial value of 0.365 to 0.29. Following one round of energy minimization and positional and B-factor refinement using 25,891 reflections from 12 to 1.8 Å resolution, (2 $|F_o|$ − $|F_c|$, α_c) and ($|F_o|$ − $|F_c|$, α_c) electron density maps were calculated. These maps revealed a large area of clear, detailed density in the active site pocket that was easily identified and fitted as the bound zopolrestat molecule. The enzyme-inhibitor model was subjected to several cycles of manual refitting of residues that undergo conformational change and modeling of ordered water molecules and positional and B-factor refinements until the R-factor converged to a final value of 0.180 at 1.8 Å resolution. The model has good geometry—r.m.s. from ideality of 0.006 Å for bonds and 1.65° for angles. It consists of 2517 atoms from the entire 315 residues, 48 coenzymes atoms, 29 zopolrestat atoms, and 175 water molecules.

Results and Discussion

The bound zopolrestat, with its very well-defined 1.8 Å difference electron density (Fig. 1 *Top*), occupies almost the entire active site pocket at the C-terminal end of the β barrel (Fig. 2). The binding has many features of a potent inhibitor. The phthalazinone ring is almost at a right angle to and bisects the plane of the benzothiazole ring (Figs. 1–3). The phthalazinone ring, protruding from the center of the pocket, is perpendicular to the nicotinamide ring of NADPH. The benzothiazole ring, lying opposite the nicotinamide ring, straddles the β barrel between strands 4 and 5 (Fig. 2). The bound inhibitor is almost completely sequestered in the cavity; it has an accessible surface area of 12.7 Å^2, 6.4% of the value for the unbound inhibitor.

There is excellent complementarity between the bound zopolrestat and the binding site. The inhibitor makes an unusually large number of contacts with the active site, totaling 132 contacts with ≤4 Å distances—110 with 15 residues, 13 with the nicotinamide moiety of the coenzyme, and 9 with 4 ordered water molecules. van der Waals contacts constitute an overwhelming number, slightly over 90%. Furthermore, as shown in Fig. 1 *Middle*, there are 9 hydrogen bonds of which 2 are long (3.7 Å) and 1 is a salt link.

About half of the van der Waals contacts are between carbon atoms, attesting to the highly hydrophobic nature of the enzyme-inhibitor interaction. Indeed, 11 apolar residues, originally found lining the active site pocket (Trp-20, Tyr-48, Trp-79, Trp-111, Phe-115, Phe-122, Trp-219, Ala-299, Leu-300, Tyr-309, and Pro-310) in the holoenzyme structure (2), are involved in these contacts. Many of these residues, especially the four residues (Trp-20, Trp-111, Phe-122, and Leu-300) that interface with the two heterocyclic rings, are shown in Figs. 1 and 3. Residue Trp-111, which stacks against the A face of the benzothiazole ring, plays a dominant role by making 38 contacts, by far the most of any residue (Figs. 1 *Top* and *Middle* and 3). The side chain of Leu-300 apposes the B face of the benzothiazole. The phthalazinone ring is sandwiched by Trp-20 and Phe-122 (Figs. 1 and 3). As these four strategically placed hydrophobic residues make 65 contacts with the inhibitor, they are major determinants of molecular recognition. The marked preference of the enzyme for hydrophobic substrates (e.g., steroids) is consistent with the mode of binding of the inhibitor.

Superpositioning of the ternary complex and holoenzyme structures reveals inhibitor-induced conformational changes of a loop (residues 121–135) and a short segment (residues 298–303) near the C-terminal end in order to accommodate and sequester the inhibitor (Fig. 3). These changes could be ascribed as hinged-flap motions. The displacement of Leu-300 as a result of inhibitor binding is accompanied by the movement of the segment 298–303 away from the pocket. Loop 121–135 moves toward the pocket, thus enabling Phe-122 to participate in inhibitor binding and to form, with Leu-300, a hydrophobic bridge over the bound inhibitor (Figs. 1 and 3). As shown in Fig. 3, several other residues contained in the loop and the segment undergo conformational changes. Moreover, the loop and the segment make favorable interactions as both slide toward each other. (These interactions are not present in the holoenzyme structure.) The superpositioned structures reveal no other similar perturbations. The formation of the hydrophobic bridge and the coalescing of the loop and segment are largely responsible in sequestering the inhibitor. It is noteworthy that the coenzyme is also strapped in place by the association of a different pair of loops that also deploy several residues that bind the coenzyme (2). Thus we have established that inhibitor and coenzyme binding induces conformational changes. It would not be surprising that substrates also possess this property.

The interaction associated with the carboxylate moiety of the inhibitor may have some bearing on enzyme catalysis. The carboxylate O3 atom, which could mimic the carbonyl oxygen of a substrate, is within very favorable distance (2.65

The C4 atom of nicotinamide ring is labeled. The following polar groups of the inhibitor (1) are recipients of a total of 9 hydrogen bonds (distances from 2.8 to 3.7 Å): O1, close to the enzyme surface, from a water molecule; O2 from His-110 Nε2H and Trp-111 Nε1H; O3 from Tyr-48 OηH and His-110 Nε2H; N2 from Cys-298 SγH; N3 from the backbone NH group of Leu-300; F1 from Thr-113 Oγ1H; and F2 from Thr-113 Oγ1H. With the exception of the long hydrogen bonds (3.7 Å) associated with N2 and F2, the others have distances between 2.8 to 3.4 Å. S1 is near Trp-111 Nε1, but the long distance (3.8 Å) and acute angle (about 90°) indicate a weak hydrogen bond between the two. A similar situation occurs between F2 and SγH of Cys-303. As the carboxylate group of the inhibitor and the side chain of His-110 are in close contact, they are also involved in a salt link. (*Bottom*) Complementary molecular surfaces between zopolrestat (green dot surface) and enzyme (red dot surface). The enzyme and inhibitor models are colored according to atom types. The nicotinamide-ribosyl-pyrophosphoryl portion of the coenzyme is shown in the lower left-hand corner. The benzothiazole ring, which is in the plane of the figure, is sandwiched by Trp-111 (below the ring) and Leu-300 (above the ring). The phthalazinone ring (perpendicular to the plane of the figure) is sandwiched between Trp-20 (left of the ring) and Phe-122 (right of the ring).

FIG. 2.   Stereo perspective view (down the C terminus of the β barrel) of the backbone trace of the structure of ALR2 with bound zopolrestat and coenzyme. The zopolrestat and coenzyme molecules are drawn as stick models, and the α helices and β strands are represented as coils and flattened arrows, respectively. The inhibitor bent at right angle is to the left of the extended coenzyme. The figure was drawn using MOLSCRIPT (14).

Å) to the oxygen of Tyr-48 OηH, which has been proposed as a proton-donor group based on the holoenzyme structure (2). The proposed function of Tyr-48 is consistent with recent site-directed mutagenesis studies (16). The O3 is at a longer distance (2.89 Å) to the nitrogen of Nε2H of His-110, another possible proton donor. The carboxylate O2 is farther away from both Tyr-48 Oη and His-110 Nε2 atoms. The C18 of the carboxylate, which would be analogous to the carbon that accepts the hydride in a substrate, is 3.63 Å of the C4 of the coenzyme.

Zopolrestat binding displaces at least six ordered water molecules found in the pocket in the 1.4 Å holoenzyme structure. This contributes favorable entropic effect to the tight binding of the inhibitor. The well-resolved, unidentified density in the active site that has been observed in both of the

FIG. 3.   Stereoview of the superimposed α-carbon backbone structures of the holoenzyme (red) and its complex with zopolrestat (green). Portions of both models (including the coenzyme) that coincide take on a yellow color. Only the region containing the loop (residues 121–135) and the segment (residues 298–303) that undergo inhibitor-induced conformational change are shown. The rest of the superimposed structures not shown are virtually identical. Several residues that undergo substantial conformational changes are also shown. The zopolrestat molecule is to the left of the nicotinamide ring of the coenzyme. The program CHAIN (15), developed in our laboratory, was used in the electron-density fitting and molecular modeling in the structure refinement and in generating Figs. 1 *Top* and *Middle* and 3.

1.4 Å and 1.65 Å (2) refined structures of the holoenzyme is no longer present in the ternary complex structure. Interestingly, we found that the portion of the unknown density closest to the nicotinamide ring coincides with the density of the carboxylate group of the bound inhibitor.

To our knowledge, none of the many potent inhibitors of ALR2 displays competitive inhibition with aldehyde as the variable substrates. Rather, these inhibitors (including zopolrestat) commonly show noncompetitive inhibition, which is likely a reflection of the following: (*i*) the sequential reaction mechanism of ALR2 with NADPH binding first (17), (*ii*) the conformational changes associated with binding and release of the coenzyme, inhibitor, and substrate, and (*iii*) the very tight affinity of the inhibitors (several with affinities 2–7 orders of magnitude greater than the K_m values of substrates). The suggestion, based on these kinetic results, that the inhibitors bind at a site that is independent of the active site (4–6), is difficult to explain in structural terms given our results showing atomic interactions between the inhibitor and the active site. Moreover, in the ternary complex structure, the active site pocket (Fig. 1) is not only completely inaccessible to solvent but also devoid of a space large enough for further productive binding of even a small substrate such as glyceraldehyde. In addition, there does not appear to be another site in the enzyme as accommodating and complementary to the inhibitor as the active site pocket.

Although the search thus far for ALR2 inhibitors has not benefited from the tertiary structure of the target enzyme, the design of zopolrestat has apparently and gratifyingly satisfied many requirements of a potent inhibitor. The structure of the ternary complex does indicate that the potency and pharmacologic requirements of this compound may be further optimized. It is also a key in rational design of new inhibitors tailored specifically for ALR2, a member of a large family of structurally and functionally related oxidoreductases.

1. Morjana, N. A. & Flynn, T. G. (1989) *J. Biol. Chem.* **264,** 2906–2911.
2. Wilson, D. K., Bohren, K. M., Gabbay, K. H. & Quiocho, F. A. (1992) *Science* **257,** 81–84.
3. Warren, J. C., Murdock, G. L., Ma, Y., Goodman, S. R. & Zimmer, W. E. (1993) *Biochemistry* **32,** 1401–1406.
4. Kador, P. F. (1988) *Med. Res. Rev.* **8,** 325–352.
5. Sarges, R. (1989) *Adv. Drug Res.* **18,** 139–175.
6. Kador, P. F. & Sharpless, N. E. (1983) *Mol. Pharmacol.* **24,** 521–531.
7. Sarges, R. & Oates, P. J. (1993) *Prog. Drug Res.* **40,** 99–161.
8. Mylari, B. L., Larson, E. R., Beyer, T. A., Zembrowski, W. J., Aldinger, C. E., Dee, M. F., Siegel, T. W. & Singleton, D. H. (1991) *J. Med. Chem.* **34,** 108–122.
9. Petrash, J. M., Harter, T. M., Devine, C. S., Olins, P. O., Bhatnagar, A., Liu, S. & Srivastava, S. K. (1992) *J. Biol. Chem.* **267,** 24833–24840.
10. Rondeau, J.-M., Tête-Favier, F., Podjarny, A., Reymann, J. M., Barth, P., Biellmann, J.-F. & Moras, D. (1992) *Nature (London)* **355,** 469–472.
11. Borhani, D. W., Harter, T. M. & Petrash, J. M. (1992) *J. Biol. Chem.* **267,** 24841–24847.
12. Rossmann, M. G. (1972) *The Molecular Replacement Method: A Collection of Papers on the Uses of Non-Crystallographic Symmetry* (Gordon and Reach, New York).
13. Brünger, A. T. (1992) x-plor: A System for Crystallography and NMR (Yale Univ. Press, New Haven, CT), 3.0 Manual.
14. Kraulis, P. J. (1991) *J. Appl. Crystallogr.* **24,** 946–950.
15. Sack, J. S. (1988) *J. Mol. Graphics* **6,** 224–245.
16. Tarle, I., Borhani, D. W., Wilson, D. K., Quiocho, F. A. & Petrash, J. M., *J. Biol. Chem.,* in press.
17. Kubiseski, T. J., Hyndman, D. J., Morjana, N. A. & Flynn, T. G. (1992) *J. Biol. Chem.* **267,** 6510–6517.